La mer 30: 95–103, 1992
Société franco-japonaise d'océanographie, Tokyo

# Meanders of the Tsushima Current

Takashi ICHIYE* and Matthew HOWARD*

**Abstract**: The Tsushima Current in the Japan Sea is treated as a thin jet in a reduced gravity field with the beta effect, including dissipation and entrainment. Integration with the latitude of a cross-jet momentum equation leads to the path equation together with the along jet momentum equation and with a simplified conservation equation of volume transport. The non-dissipative and transport conserved solution corresponds to the one derived by C.G.ROSSBY and R.O.REID earlier. The linear friction and a given entrainment function are incorporated in a linearized form. Those effects tend to cause crossings of the streamlines, suggesting that these processes may be a cause of pinch-off of mesoscale eddies frequently observed in the Japan Sea. As preliminary applications, several computed paths are fitted to the 100m isotherms of the Japan Sea collected in August 1990. An example of meso-scale eddies formation by streamline crossing is inferred from a series of IR images taken in spring of 1984 west of Oki Island.

## 1. Introduction

Meandering of the Tsushima Current (TC) can be seen in charts of isotherms both at the surface and subsurface published routinely by the Japan Meteorological Agency, Hydrographic Department of the Maritime Safety Agency and the Japan Fisheries Agency. The 100m isotherms are particularly useful to interpret the meander from ocean dynamics, because they are relatively free from short-term interactions by the atmospheric heating. They represent to a degree geostrophic flow in the upper layer (ICHIYE and TAKANO, 1988) and the data are relatively abundant.

Many Japanese authors noticed that in the Japan Sea the water below 200–300 meters is almost uniform both in temperature and salinity with a sharp thermocline and pycnocline at these levels (MORIYASU, 1972; KAWABE, 1982). This feature suggests that we can handle dynamics of the TC that mainly flows in the upper 200m as a process in a two-layer ocean with an inactive lower layer. This does not imply that effects of the lower layer or bottom topography are unimportant to the TC. On the contrary, these effects could become important for long-term behaviors of the TC and their effects on heat and mass transports in the Japan Sea.

In this paper we only deal with a short-term or synoptic process with the duration of, say several weeks but after achieving geostrophic adjustment. A basic approach is to start from momentum equations with natural coordinates, incorporating the conservation of volume in a simple scheme with an assumption that the TC is a jet-like flow with almost uniform across the flow. Emphasis is put on paths of the flow as it meanders in the upper layer.

## 2. Basic equations

The natural coordinates ($s$, $n$) are taken with $s$ along the flow and $n$ across it to the left, as indicated in Fig. 1. The momentum conservation equations along $s$ and $n$ are given by

$$v\frac{\partial v}{\partial s}=-g'\frac{\partial h}{\partial s}-F \qquad (1)$$

$$\kappa v^2+fv=-g'\frac{\partial h}{\partial n} \qquad (2)$$

respectively, where $v$, $h$, $\kappa$, $f$, $g'$, and $F$ are velocity, thickness of the upper layer, curvature of streamlines, Coriolis parameter, reduced gravity and dissipation force, respectively.

Conservation of volume transport is expressed by

* Department of Oceanography, Texas A & M University, College Station, Texas 77843 USA

$$vh=v_0h_0+S \tag{3}$$

S is the entrainment (or detrainment) along the flow and the suffix o indicates the values at the starting point (for the TC at the Korean Strait). More exactly, both sides should be averaged across the flow over an unspecified width, but this analytical subtlety is forsaken for conceptual simplicity of (3). If we assume that the velocity vanishes outside a narrow band of the flow and that there is no dissipation and entrainment then equation (1) yields

$$\frac{1}{2}v^2+g'h=\frac{1}{2}v_0^2+g'h_0-G \tag{4}$$

This equation represents the energy conservation along a streamline and this equation with $G=0$ and equation (3) with $S=0$ leads to a solution

$$v=v_0, \quad h=h_0 \tag{5}$$

Therefore, both $v$ and $h$ are constant along the streamline, equaling their initial values, though they may be variable across the flow. By solving equations (3) and (4) as algebraic equations about $v$ and $h$, these two quantities can be determined in terms of $v_0$, $h_0$, $S$ and $G$, where $v_0$ and $h_0$ are dependent on $n$ only but $S$ and $G$ are dependent on both $n$ and $s$. Equations (3) and (4) lead to a cubic equation about $v$ or $h$ which has three roots. One of the roots is positive and equivalent to (5) even when $G$ and $S$ do not vanish. When there is a root which is real and positive, two or three roots can represent real flows. In ICHIYE (1990), it was speculated that transition from one flow regime represented by one root to other regime represented by another root could be occurred analogous to hydraulic jumps in a channel flow when the streamlines crossed each other. Such processes seem to be a cause of mushroom-like flows, particularly of multiple structures which had been observed commonly along the edge of a jet-like flow of warm water or fresher water over heavier stagnant water of a great depth below (FEBROV and GINSBURG, 1989).

In other manifests of streamline crossings and transitions in flow regimes can be seen in IR images of the Tsushima Current west of Oki Island. KITANI *et al.* (1986) analyzed IR data from March 28 to April 24, 1984 and reported formation and change of warm water belts of 10 to 20 km wide and 100 to 200 km long at about 132° E to 133° E and 36° N to 38° N. The location of these belts corresponds to the west leg of the second penetration of the meander (west of a portion designated C in Fig. 8). The tip of the warm belts indicated anti-cyclonic vorticity. The formation took only 12 hours in the beginning but for full development it took several days.

Since the location of formation of the warm belts or ribbons could be determined with IR imagery and its time scales are within range of shipboard measurements, it is possible to determine dynamical processes accompanying with streamline crossing and the transition of flow regimes corresponding to different roots of equation (3) and (4). The results of further studies on this problem will be reported elsewhere.

Since the TC flows from 35° N to 45° N, the beta effect cannot be neglected as in ICHIYE (1990) , where $G$ and $S$ are assumed to vanish. The $x-y$ coordinates are taken as eastward and northward (Fig. 1). Then the curvature can be expressed by

$$\kappa = \frac{\partial \theta}{\partial s} \tag{6}$$

where $\theta$ is the angle of the streamline with the $x$-axis. When the effects of dissipation and entrainment are small, deviation of $v$ and $h$ from $v_0$ and $h_0$ are also small. Thus

$$v=v_0+a, \quad h=h_0+b \tag{7}$$

When at the starting point ($s=0$ and $y=0$) the flow is geostrophic,

$$f_0=-\left(\frac{g'}{v_0}\right)\frac{\partial h_0}{\partial n} \tag{8}$$

Using a relation $\partial y/\partial s=\sin\theta$ in (6), equation (2) can be integrated with $\theta$ and $y$, leading to

$$\cos\theta-\cos\theta_0=\int_0^y\left(fv^{-1}+g'v^{-2}\frac{\partial h}{\partial n}\right)dy \tag{9}$$

Anomalies $a$ and $b$ can be determined by substituting (7) into (3) and (4). When only the first order terms of $a$ and $b$ are retained,

$$a=(v_0G+g'S)\,q^{-1} \tag{10a}$$
$$b=-(h_0G+v_0S)\,q^{-1} \tag{10b}$$

where

$$q=g'h_0-v_0^2 \tag{11}$$

When (7) is substituted into (9), retaining only the first order terms of $a$ and $b$ and relation (8) is used, (9) becomes

$$\cos\theta=\int_0^y\left[\beta y v_0^{-1}+a(f_0-\beta y)v_0^{-2}+g'\left(\frac{\partial b}{\partial n}\right)v_0^{-2}\right]dy \tag{12}$$

where the relation $f=f_0+\beta y$ is used, $v_0$ is constant and the flow at the starting point is assumed northward ($\theta_0=\pi/2$).

The dissipation term $G$ is an integration of frictional force $F$ along the path. In a simple parameterzaion, we assume Rayleigh-type frictional force and also the path mainly of meridional direction. Then

$$G=kv_0y \tag{13}$$

where $k$ is a friction coefficient including a factor of deviation of the path from the strictly meridional direction. Substitution of (10) and (13) into (12) leads to

$$\cos\theta=g'f_0Sq^{-1}(v_0^{-2}-q^{-1})y+\frac{1}{2}(v_0^{-1}\beta+2kf_0q^{-1}-g'kf_0h_0q^{-2}v_0^{-1}-g'Sq^{-1}\beta v_0^{-2})\,y^2-\frac{k\beta}{qv_0}\frac{y^3}{3} \tag{14}$$

As expected the terms with $S$ represent the effects of entrainment and those with $k$ indicate effects of friction. Since only the first order term of $a$ and $b$ are retained, the friction and the entrainment are affecting the path independently. A case of $k=0$ and $S=0$ corresponds to a path obtained by REID (1968) as it should be. In the present derivation, we do not use the rule of conservation of potential vorticity. In ICHIYE (1990) this rule is derived from equations (2) and (3) with $S=0$ and (4) with $G=0$.

Admittedly the assumption that the entrainment function $S$ and a frictional force $F$ are independent on $s$ is very crude indeed, though $S$ and $k$ could be assigned functions of $n$. (It is unwarranted to assume $S$ as a linear function of $y$ similar to (13) as suggested by $a$, reviewer, because relation (3) specifies volume transport at each section represented by $s$, unlike $G$ that is an integral of $F$ along the path.) Of course, $S$ could be taken as an arbitrary function on both $n$ and $s$ in equation (14) and determined the path or, by fitting the path to the observed path and determine $S$ as a function of $n$ and $s$. But in the present stage of uncertainties in the information on various parameters, these exercises seem to complicate modelling unnecessarily.

## 3. Numerical calculation

The path can be determined from the relation

$$dx/dy=\cot\theta \tag{15}$$

where the r.h.s. can be obtained from (14). Although $v_0$ is assumed constant, $h_0$ and $S$ are variable with $n$; therefore $\theta$ is dependent on $n$. Thus the streamlines are not necessarily parallel to each other and they may diverge, or converge and even cross each other, particularly when $S$ is not zero.

For numerical calculation, the r.h.s. of equation (14) is scaled with characteristic values. $l_h$, $h_b$, $h_m$, and $v_1$ which are horizontal distance, right hand side depth and mean depth of the flow at the starting point, and speed, respectively. For simplicity, the initial speed is constant; thus from (8)

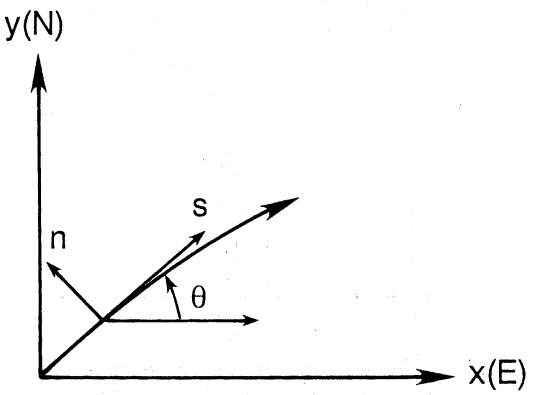


Fig. 1. Natural coordinate system with Cartesian coordinates.

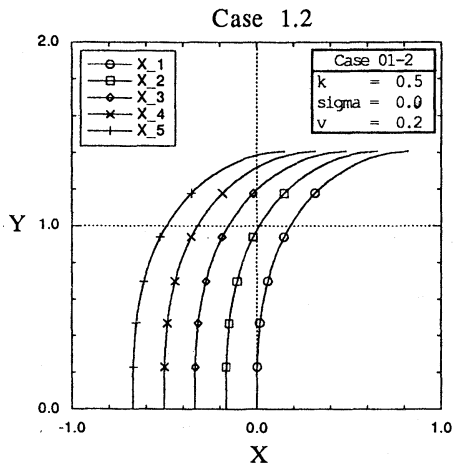


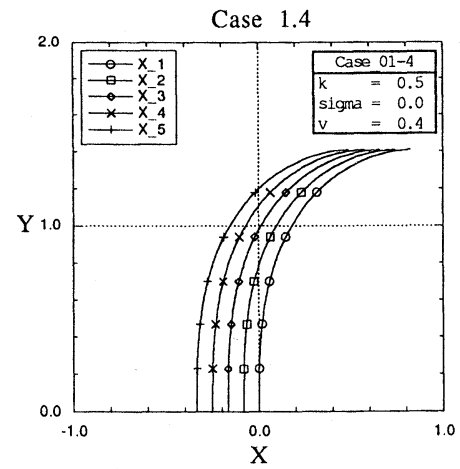


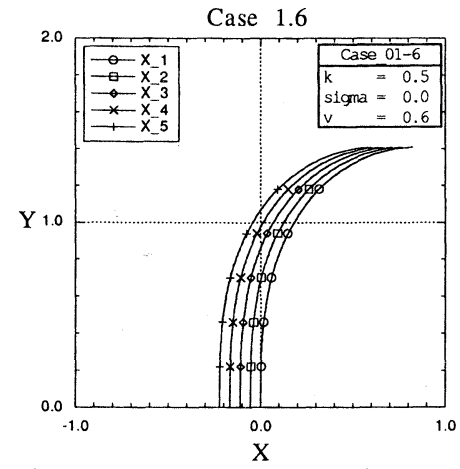


Fig. 2. Three examples of streamlines computed from equations (18) to (20). For $K$=0.5 and $V$=0.2 to 0.6. The streamlines converge but not cross each other.

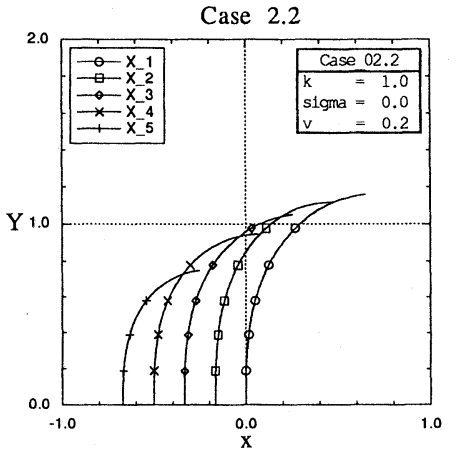


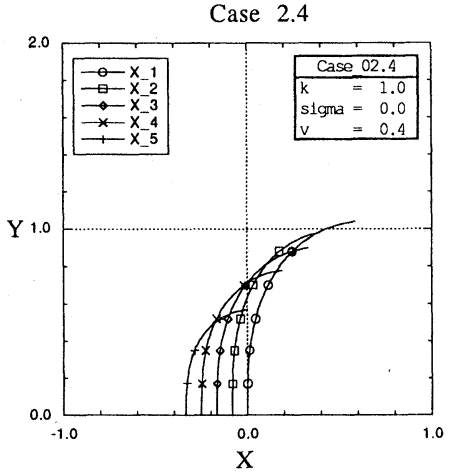


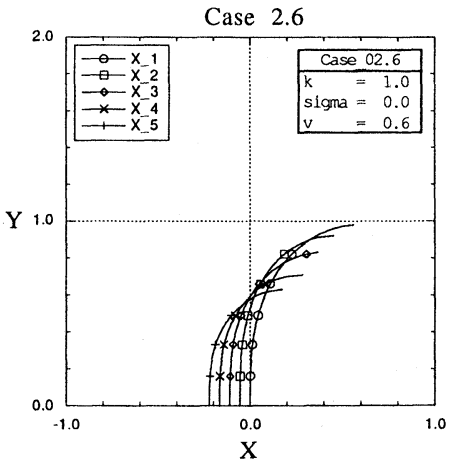


Fig. 3. Three examples of computed streamlines, for $K$=1.0 and $V$=0.2 to 0.6. The streamlines cross each other.

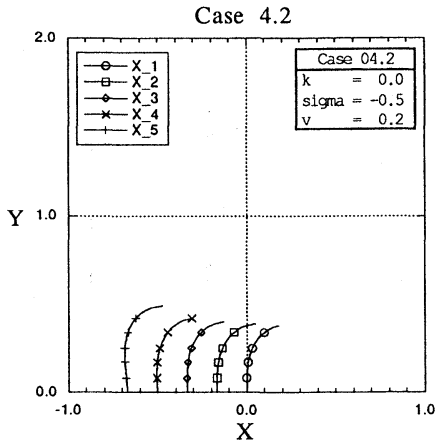


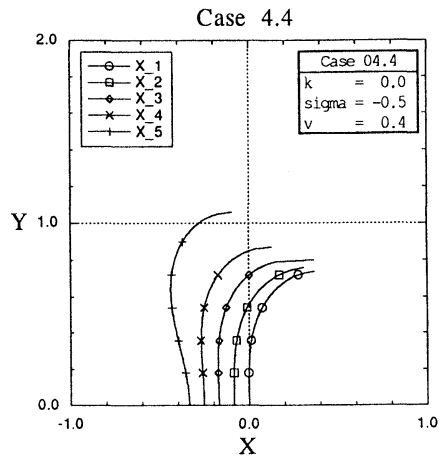


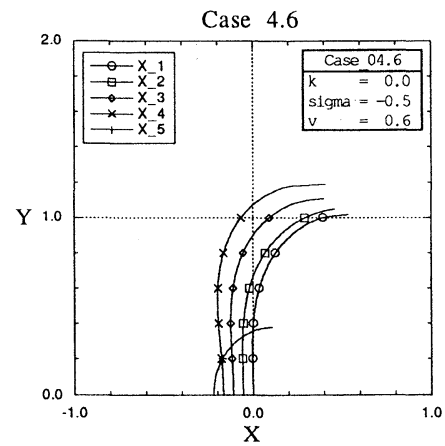


Fig. 4. Three examples of computed streamlines, for $\sigma = -0.5$, corresponding detrainment along the path. The streamlines do not reach as cases of no entrainment or detrainment. Some streamlines cross near the starting point in case for $V$=0.6

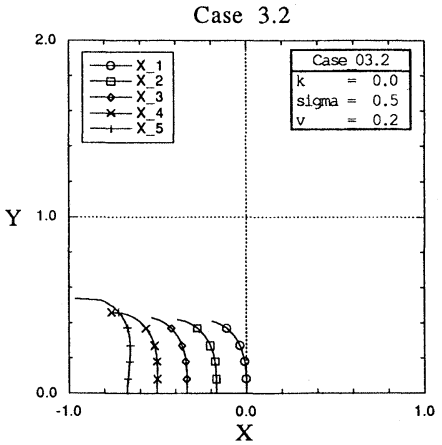


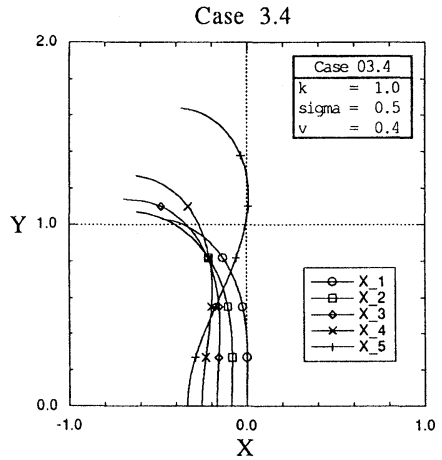


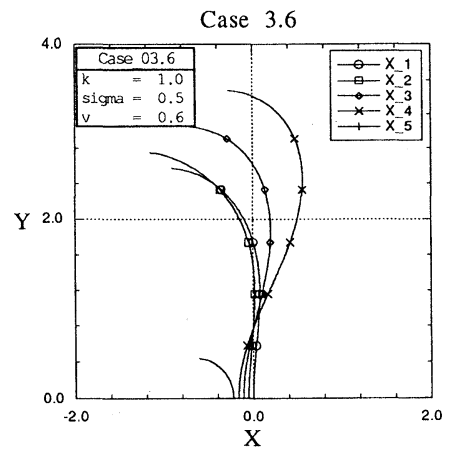


Fig. 5. Three examples of computed streamlines for $\sigma = 0.5$, corresponding to entrainment. Entrainment cause streamlines becoming cyclonic and also crossing each other for faster speed.

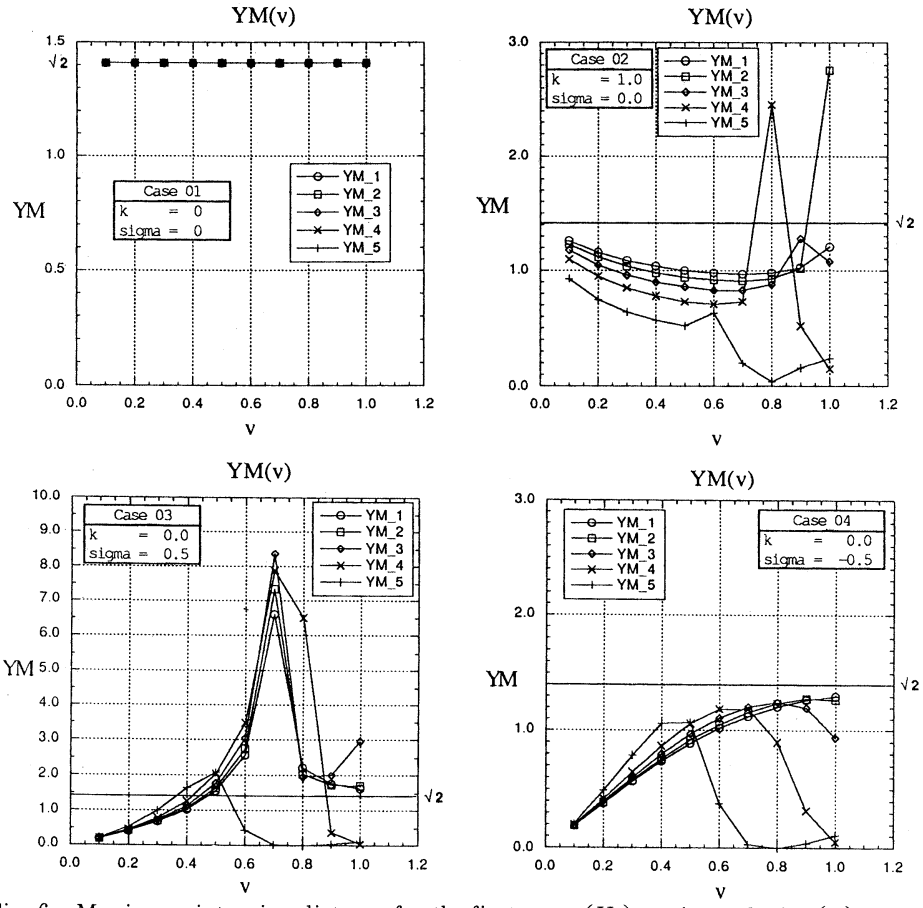


Fig. 6. Maximum intrusion distance for the first wave ($Y_m$) against velocity ($V$) for different streamlines with different combinations of $K$ and sigma. YM-1 etc. correspond to streamlines at different starting points denoted as X-1 etc. in Figs. 2 to 5. Crossings of $Y_m$ versus $V$ curve indicate crossings of the streamlines for which $Y_m$ is computed. The figure shows that with non-zero sigma values (entrainment) streamlines tend to cross each other for smaller $V$ than for cases with dissipation only.

$$h_0 = h_b + (f_0 v_0 / g')x \tag{16}$$

Then

$$l_h = (v_0/\beta)^{1/2},\ v_0 = v_1 V,\ h_0 = h_b H,\ x = l_h X,$$
$$y = l_h Y,\ q = v_0^2 Q,\ k = k_0 K,\ S = \sigma v_1 h_m \tag{17}$$

where $H$, $V$, $Q$, $X$, $K$, and $\sigma$ are dimensionless parameters and variables.

When the following values are used for characteristic parameters, $v_0 = 1\,\mathrm{ms}^{-1}$; $\beta = 2 \times 10^{-11}\,\mathrm{m}^{-1}\mathrm{s}^{-1}$; $f_0 = 8 \times 10^{-5}\,\mathrm{s}^{-1}$; $h_m = 75\mathrm{m}$; $h_b = 150\mathrm{m}$; $k_0 = 10^{-6}\,\mathrm{s}^{-1}$, equations (14) and (16) can be expressed by

$$\cos\theta = 2.0035 Q^{-1}(1-Q^{-1})\,\sigma V^{-5/2} Y + (1 + 8Q^{-1}KV^{-1} - 12HKV^{-2}Q^{-2} - 1.12\,\sigma V^{-2})\frac{1}{2}Y^2 - 0.0527\,Q^{-1}Y^3 KV^{-1/2} \tag{18}$$

and

$$H = 1 + 5.963\,V^{3/2}X_0 \tag{19}$$

where

$$Q = V^{-2}(3H - V^2) \tag{20}$$

In equation (19), $X_0$ indicates the starting

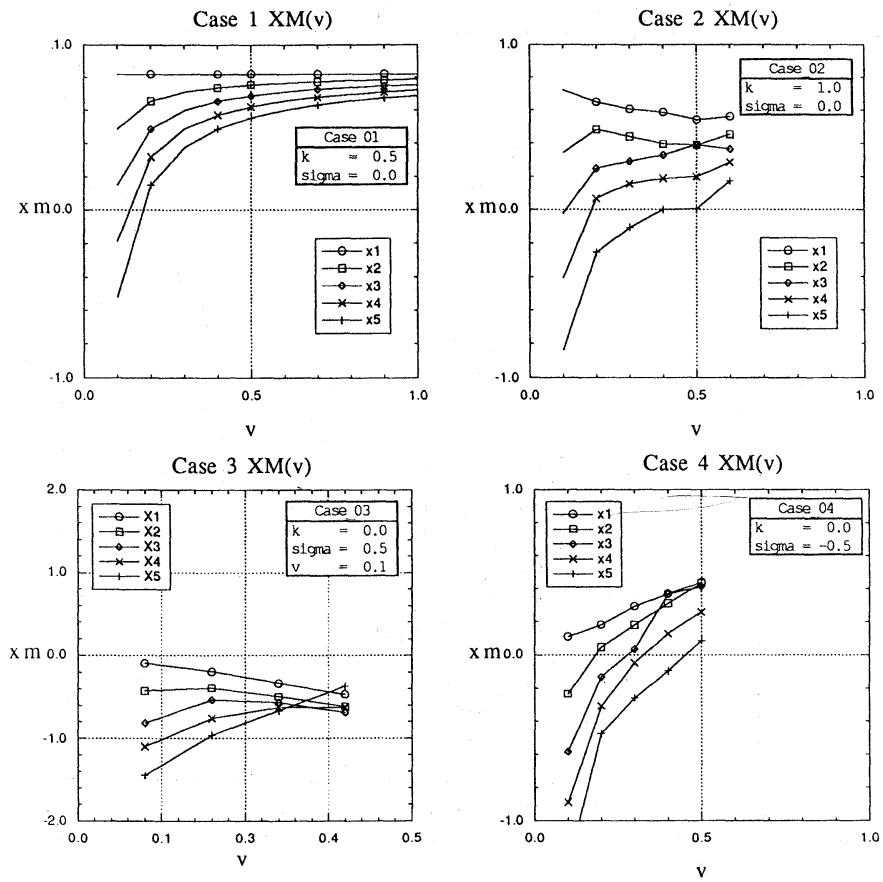


Fig. 7. $X_m$ corresponding to $Y_m$ as determined in Fig. 6. The $X_m$ values indicate those on the $X$ coordinate as in Figs. 2 to 5. The distance of the quarter wave length in zonal direction of each streamline can be determined by subtracting the initial $X$ coordinate denoted as X-1, X-2 etc. in Figs. 2 to 5 from curves of $X_m$ ($V$) in this figure. (For example streamline X-5 at $V=0.2$ $K=1$ has $X_m=-0.3$ and the starting point $X$ coordinate is $=-0.7$. Thus the quarter wave length is about 0.4).

position of each streamline and thus can be treated as a parameter for integrating equation (15) with $Y$ by replacing $\partial x/\partial y$ with $\partial X/\partial Y$. The mean value $h_m$ is taken for an initial flow in which the thermocline surfaces at the left hand side.

Several examples of the path determined from (18) to (20) are shown in the $X$-$Y$ coordinates in Fig. 2 to 5 for different value of $\sigma$ and $K$. With inclusion of small entrainment or detrainment ($\sigma$ is non-zero), the path sometimes changes drastically.

Equations (14) or (20) indicate that the path determined from(15)or its equivalent expression with $X$ and $Y$ shows a wave form extending eastward as expressed in general with elliptic integrals on $y$ or $Y$. The northernmost intrusion of the first wave denoted as $Y_m$ can be determined as the first $Y$ satisfying $\cos\theta=1$. The value $X_m$ corresponding to $Y_m$ on the path is equivalent to a quarter of the wavelength. Figures 6 and 7 show values of $Y_m$ and $X_m$ for different values of $V$ at different values of $K$ and $\sigma$.

## 4. Application to the Tsushima Current paths

Isotherms at 100 m are plotted in Fig.8 from data collected by about a dozen research vessels and patrol boats from August 1 through August 15, 1990 (Japan Fisheries Agency, 1990).

For a non-dissipation non-entrainment case,

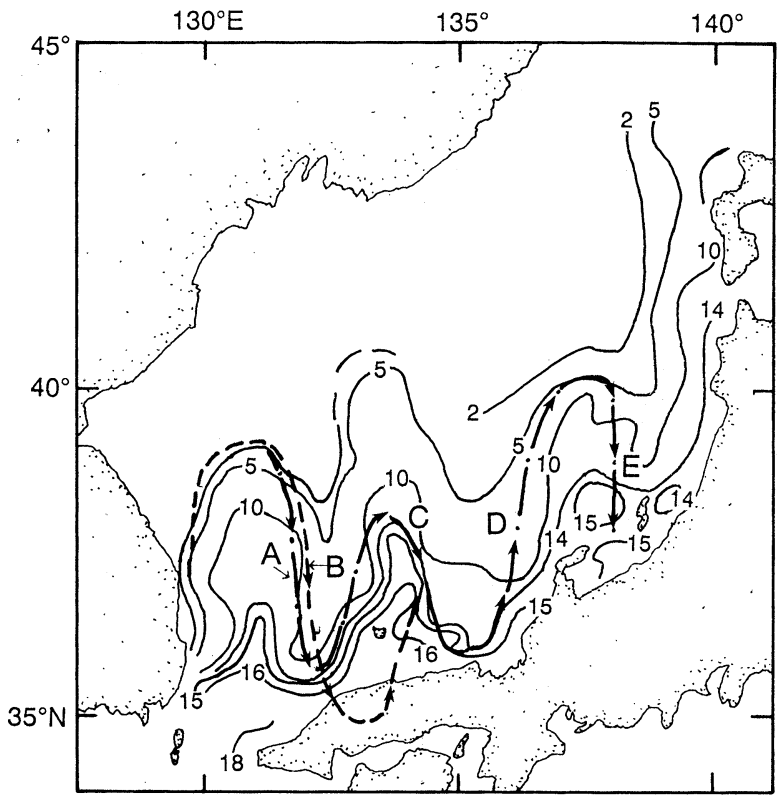


Fig. 8. Example of comparison of 100 m isotherms and computed paths in the Japan Sea. Isotherms are labeled in ℃ and based on data of Fishing Ground Oceanography Charts for August 1990. (Japan Fisheries Agency).

Dashed line denoted B represents the path for no dissipation, no entrainment case with $V=0.5$. Dash-dot line represents the path including non-zero $K$ or $\sigma$. Different segments of the dash-dot line are labeled according the the following specifications: A, $\sigma=0.2$; C, $K=0.5$; D, $\sigma=0.5$; E, $\sigma=-0.2$.

the speed $V=0.5$ or $v_0=0.5\mathrm{ms}^{-1}$ seems to be best fit to the first wave of the northward intrusion of the observed isotherm meander. However, the theoretical curve does not fit the second wave crest around 133° E. Third wave is completely out of phase from the theoretical curve. This is due to the condition that the second trough (or southward retreat) interacts strongly with the shelf or the coastline as seen from the figure.

## 5. Concluding remarks

This is a preliminary study of dynamics of meanders of the Tsushima Current. As shown in Fig.8 modelled paths of the meander are deviated after the first intrusion approaches the coast on its retreat. This suggests both dissipative and entrainment processes are admittedly parameterized inadequately.

This could be improved substantially with help of field experiments that are to be addressed to the dissipative processes in shallow water areas less than 200m and to the entrainment processes in similar areas from coastal water. These experiments may be made successfully with conventional hydrographic techniques if the experimental cruises are planned carefully.

Crossings of the streamlines occur for the flow with $v_0$ and $h_0$ that are not uniform across the section (dependent on $n$) as shown in the case of $S$ and $G=0$ (ICHIYE, 1990). When $S$ and $G$ do not vanish, further upstream these crossings are apt to occur in the path of the flow than when $S=G=0$, since finite $S$ or $G$ makes $h$ and $v$

deviate from uniform and become dependent on $n$.

Crossings with or without dissipation or entrainment suggest formation of mesoscale eddies in the Japan Sea as pointed out by ICHIYE and TAKANO (1988). Influence of dissipation and entrainment on crossings indicates necessity to parameterize these processes more adequately particularly upstream of the crossings or eddy formation. Since locations of the latter processes manifested as warm water ribbons were known at least west of Oki Island, it is not difficult to conduct field experiments with drifters, closely spaced CTD measurements and moored current meters by coordinating ongoing studies of the Tsushima Current by several agencies and institution. Then the results might shed light on dynamics of crossings of streamlines, transition of flow regimes caused by different roots of (3) and (4) as well as mechanism of formation of mesoscale eddies from a jet-like ocean current, that is so ubiquitous in the world ocean but yet to be understood its physics.

**Acknowledgement**

The second author is supported by U.S.W.O.C.E. program. Typing by Susan MAHAN is appreciated.

**References**

FEDROV, K.N. and A.I. GINSBURG (1989): "Mushroom like" currents: one of the most widespread forms of non-stationary motion in the oceans. Geophysical Turbulence, Proc. 20th Liege Colloq. on Ocean Hydrodynamics. (edited by J.C.J. NIHOUL and B.M. JAMART) 1–14, Elsevier Publishers, 844pp.

ICHIYE, T. (1990) : A simple model of mushroom-like flows. Tribute to Prof. K.N.FEDROV, Pacific Annual, 1989–1990 (Far Eastern Branch, USSR Academy of Sciences, Vladivostok), 131–145.

ICHIYE, T. and K. TAKANO (1988): Mesoscale eddies in the Japan Sea. La mer, **26**, 69–79.

KAWABE, M., (1982): Branching of the Tsuhima Current in the Japan Sea I and II. J. Oceanogr. Soc. of Japan, **38**, 95–107, 183–192.

KITANI, K., H. NAGATA and K. MUNEYAMA (1986): An explanation of the sea condition off San-In District based on infrared images. Sora To Umi (in Japanese) No. 8, 15–25.

MORIYASU, S. (1972): The Tsushima Current. Chapt. 9, 353–369. *In* The Kuroshio, Its Physical Aspect, (Edited by H. STOMMEL and K. YOSHIDA), Univ. of Tokyo Press, 517p.

REID, R.O. (1972): A simple dynamic model of the Loop Current. 157–159, Contributions on the Physical Oceanography of the Gulf of Mexico, (edited by L.R.A. CAPURRO and J.L. REID), Gulf Publishing Co., Houston, Texas, 288p.

ROSSBY, C.G. (1945): On the propagation of frequencies and energy in certain types of oceanic and atmospheric waves. J. Meteorol. **2**, 187–204. Also *in* Handbook of Meteorology (edited by F.A. BERRY, E. BOLLAY and N.R. BEERS), McGRAW Hill Inc., New York, (1945).